

A new class of light absorber–electron acceptor dyad

Lisa M. Vrana, Karen J. Brewer *

Department of Chemistry, Virginia Polytechnic Institute and State University, Blacksburg, VA 24061-0212, USA

Received 8 May 1996; revised 20 August 1996

Abstract

The ligand 2,3,5,6-tetrakis(2-pyridyl)pyrazine (tpp) can be used to bind to one or two metal centers. When this ligand is bound in a tridentate fashion to a single metal, three remote nitrogens remain, which are uncoordinated. Methylation of one of the pyridine nitrogens is possible in high yield to form a covalently coupled viologen. This viologen functions as an electron acceptor to form the basis of a molecular dyad composed of a light absorber–electron acceptor framework. Two such dyads have been synthesized utilizing the other polypyridine ligands 2,2'-bipyridine (bpy) and 2,2':6',2''-terpyridine (tpy). The spectroscopic, electrochemical and photochemical properties of these dyads, $[\text{Ru}(\text{tpy})(\text{Metpp})]^{3+}$ and $[\text{Ru}(\text{bpy})(\text{Metpp})(\text{CH}_3\text{CN})]^{3+}$, as well as the unmethylated analogs, $[\text{Ru}(\text{tpy})(\text{tpp})]^{2+}$ and $[\text{Ru}(\text{bpy})(\text{tpp})(\text{CH}_3\text{CN})]^{2+}$, have been studied (Metpp, 2-[2-(1-methylpyridinium)]-3,5,6-tris(2-pyridyl)pyrazine). Electrochemically, in the unmethylated complexes, we observe an Ru(II)/Ru(III) oxidation and a tpp/tpp⁻ reduction, which is localized on the pyrazine portion of tpp. On methylation, the ruthenium metal becomes slightly harder to oxidize and a new reduction appears prior to the reduction of the pyrazine ring of the Metpp ligand. This can be attributed to the reduction of the viologen portion of Metpp. Optical excitation of the methylated complex is similar to that of the unmethylated species, with the lowest lying spectroscopically accessible excited state involving Ru(dπ) → tpp(π*) charge transfer with the acceptor orbital being largely localized on the pyrazine portion of the tpp ligand. The lowest unoccupied molecular orbital in the methylated complexes resides on the viologen portion of the Metpp ligand, making these complexes light absorber–electron acceptor dyads. © 1997 Elsevier Science S.A.

Keywords: Light absorber–electron acceptor dyad; 2-[2-(1-Methylpyridinium)]-3,5,6-tris(2-pyridyl)pyrazine; 2,3,5,6-Tetrakis(2-pyridyl)pyrazine

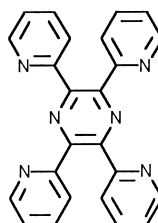
1. Introduction

In the early 1970s, it was realized that the metal-to-ligand charge transfer (MLCT) excited states of ruthenium polypyridine complexes could be involved in bimolecular energy and electron transfer processes [1–11]. Such complexes possess easily tunable redox properties, making them ideal components for excited state electron transfer reactions. Recent interest has focused on the covalent coupling of electron donors and electron acceptors to these and other types of chromophore [12–34]. In addition, much interest has focused on polymetallic systems linked together by bridging ligands [35–51].

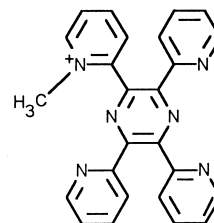
In 1992, Serroni and Denti [52] devised a protection/deprotection sequence for use in the construction of multi-metallic complexes containing the ligand 2,3-bis(2-pyridyl)pyrazine (dpp). They followed a stepwise procedure in which the ligand was singly methylated to protect one coordination site. This ligand was then bound to a metal center and the methyl group was removed, deprotecting the site, making it available for the coordination of another metal

center. This procedure was used to synthesize larger supra-molecular systems.

The addition of a methyl group to a polypyridyl ligand on the pyridyl nitrogen leads to the formation of a viologen and thus should allow the ligand to act as an electron acceptor [34,52]. If this can be accomplished using a ligand in which the remote pyridine is not involved in the optically populated state, a new type of covalently coupled electron acceptor could be designed. Brewer et al. [49] have shown that the ligand 2,3,5,6-tetrakis(2-pyridyl)pyrazine (tpp) has a π* lowest unoccupied molecular orbital (LUMO) which is largely localized on the pyrazine portion of the ligand.



tpp



Metpp

* Corresponding author.

Hence the methylation of a pyridine should form a new ligand, 2-[2-(1-methylpyridinium)]-3,5,6-tris(2-pyridyl)-pyrazine (Metpp), in which optical excitation can still occur to the acceptor π^* orbital on the pyrazine, but intramolecular electron transfer quenching of this optically populated state can produce a reduced viologen.

In this study, we have synthesized two ruthenium systems incorporating our new covalently coupled electron acceptor. A comparison of the properties of the methylated complexes, [Ru(tpy)(Metpp)](PF₆)₃ and [Ru(bpy)(Metpp)(CH₃CN)](PF₆)₃, with those of the unmethylated analogs, [Ru(tpy)(tpp)](PF₆)₂ and [Ru(bpy)(tpp)(CH₃CN)](PF₆)₂, is made. Electronic absorption spectroscopy, electrochemistry, spectroelectrochemistry, emission spectroscopy and excited state lifetime measurements were used in the analysis of these systems.

2. Experimental details

2.1. Materials

All chemicals were of reagent grade and were used without further purification. Ruthenium trichloride was received through the Johnson Matthey precious metal loan program. The ligand 2,2':6',2''-terpyridine (tpy) and trimethyloxoniumtetrafluoroborate [(CH₃)₃OBF₄] were purchased from Aldrich Chemical Company. The ligand tpp was purchased from GFS Chemicals. The acetonitrile used in the spectroscopic and electrochemical studies was Burdick and Jackson UV grade.

2.2. Synthesis

Ru(tpy)Cl₃ [53], [Ru(tpy)(tpp)](PF₆)₂ [50,54,55] and Ru(bpy)Cl₄ [56] were prepared according to published methods. All reactions were carried out under argon.

2.2.1. {2-[2-(1-Methylpyridinium)]-3,5,6-tris(2-pyridyl)-pyrazine}(2,2':6',2''-terpyridine)ruthenium(II) hexafluorophosphate ([Ru(tpy)(Metpp)](PF₆)₃)

This can be prepared by two different methods, both using trimethyloxoniumtetrafluoroborate as the methylating agent. The first method is a modification of the procedure used by Serroni and Denti [52] to methylate dpp in the preparation of multimetallic systems. [Ru(tpy)(Metpp)]³⁺ was synthesized by adding [Ru(tpy)(tpp)]²⁺ (0.098 g, 0.11 mmol) and (CH₃)₃OBF₄ (0.052 g, 0.35 mmol) to 50 ml of 1,2-dichloroethane. This was heated at reflux and stirred for 3 h under argon. The product was separated by vacuum filtration. Purification was performed by column chromatography on adsorption alumina in 3 : 2 (v/v) acetonitrile–toluene solvent mixture. The first band to elute (light orange) was unreacted [Ru(tpy)(tpp)]²⁺ and the second band (a darker orange), which contained the product of interest, eluted when a 2 : 1 (v/v) acetonitrile–methanol solution was used. This

fraction was collected, concentrated by rotary evaporation, dissolved in a minimum amount of acetonitrile and flash precipitated in diethyl ether. The product was separated by vacuum filtration and dried under vacuum. A typical yield for this reaction was 32%.

The second method was similar in design, but gave an improved yield. The methylated complex was prepared by adding (CH₃)₃OBF₄ (0.012 g, 0.081 mmol) and [Ru(tpy)(tpp)](PF₆)₂ (0.070 g, 0.069 mmol) to a 100 ml, three-necked, round-bottomed flask fitted with an argon inlet. Using a syringe, 50 ml of distilled dichloromethane was added to the mixture. This was heated at reflux with stirring under argon for approximately 3 h, and then cooled to room temperature. The solid was isolated by vacuum filtration and purified as described above. A typical yield for this reaction was 71%.

2.2.2. (2,2'-Bipyridine)chloro(2,3,5,6-tetrakis(2-pyridyl)-pyrazine)ruthenium(II) hexafluorophosphate

To Ru(bpy)Cl₄ (0.152 g, 0.381 mmol) and tpp (0.185 g, 0.477 mmol) was added 40 ml of 1 : 1 (v/v) ethanol–water solution and 2 ml of triethylamine. This was refluxed with stirring under argon for 4 h, and then cooled to room temperature. The crude product formed by addition to a saturated aqueous solution of KPF₆ was separated through vacuum filtration and purified by column chromatography on adsorption alumina using 2 : 1 (v/v) toluene–acetonitrile solution as eluent. The first band to elute was tpp starting material. [Ru(bpy)(tpp)Cl](PF₆), the red band, was the second to elute. This fraction was collected, concentrated by rotary evaporation, dissolved in a minimum amount of acetonitrile and flash precipitated in diethyl ether. The product was separated by vacuum filtration and dried under vacuum. The chromatographic purification was repeated twice to ensure product purity. A typical yield for this reaction was 83%.

2.2.3. Acetonitrile(2,2'-bipyridine)(2,3,5,6-tetrakis(2-pyridyl)pyrazine)ruthenium(II) hexafluorophosphate

A solution of [Ru(bpy)(tpp)Cl]⁺ (0.104 g, 0.126 mmol) and a large excess of AgPF₆ (0.319 g, 1.26 mmol) in 25 ml of acetonitrile and 25 ml of water was heated at reflux with stirring for 6 h under argon. The AgCl was removed by vacuum filtration and the acetonitrile was removed by rotary evaporation. On addition to an aqueous solution of saturated KPF₆, a precipitate was obtained, removed by vacuum filtration and purified by alumina adsorption chromatography using 1 : 1 (v/v) toluene–acetonitrile as eluent. The first band to elute was unreacted [Ru(bpy)(tpp)Cl]⁺. The second band to elute was yellow [Ru(bpy)(tpp)(CH₃CN)](PF₆)₂. This fraction was collected, concentrated by rotary evaporation, dissolved in a minimum amount of acetonitrile and flash precipitated in diethyl ether. The solid was separated by vacuum filtration and dried under vacuum. A typical yield for this reaction was 95%.

2.2.4. Acetonitrile(2,2'-bipyridine){2-[2-(1-methylpyridinium)]-3,5,6-tris(2-pyridyl)pyrazine}ruthenium(II) hexafluorophosphate

The methylation of $[\text{Ru}(\text{bpy})(\text{tpp})(\text{CH}_3\text{CN})](\text{PF}_6)_2$ was achieved following the procedure for the methylation of $[\text{Ru}(\text{bpy})(\text{tpp})]^{2+}$. To $[\text{Ru}(\text{bpy})(\text{tpp})(\text{CH}_3\text{CN})]^{2+}$ (0.48 g, 0.049 mmol) and $(\text{CH}_3)_3\text{OBF}_4$ (0.028 g, 0.19 mmol) was added 50 ml of distilled dichloromethane. The mixture was heated at reflux and stirred under argon for 3 h. The solid was collected by vacuum filtration and purified by alumina adsorption chromatography using 3 : 2 (v/v) acetonitrile–toluene solution. The first band to elute was the unreacted starting metal complex, whereas the second band was the methylated complex $[\text{Ru}(\text{bpy})(\text{Metpp})(\text{CH}_3\text{CN})](\text{PF}_6)_3$. This fraction was collected, concentrated by rotary evaporation, dissolved in a minimum amount of acetonitrile and flash precipitated in diethyl ether. The product was separated by vacuum filtration and dried under vacuum. A typical yield for this reaction was 80%.

2.3. Electronic absorption spectroscopy

Absorption spectra were recorded at room temperature in Burdick and Jackson acetonitrile on a Hewlett Packard 8452A diode array spectrophotometer (resolution, 2 nm).

2.4. Emission spectroscopy

Emission spectra were recorded at room temperature in deoxygenated Burdick and Jackson acetonitrile solution. They were obtained on a Photon Technology International Inc. Alphascan system, using a 150 W mercury arc lamp as excitation source and a thermoelectrically cooled Hamamatsu R666-S photomultiplier tube with single-photon counting detection. In general, 15 scans were repeated and averaged. All spectra were corrected for the photomultiplier response. Low-temperature emission spectra were recorded on deoxygenated, absorbance-matched ethanol solutions prepared in quartz tubes using an optical Dewar containing liquid nitrogen.

2.5. Excited state lifetime measurements

Excited state lifetime measurements were obtained using a Photon Technology International Inc. PL 2300 nitrogen laser equipped with a PL 201 continuously tunable dye laser (360–900 nm) as excitation source. The excitation pulse was passed through an optical trigger prior to entering the sample compartment. The emission from the excited state was detected at right angles. The emission was passed through a PTI 1200 lines mm^{-1} grating monochromator and detected by a Hamamatsu R928 photomultiplier tube. Solutions for the excited state lifetime measurements were prepared using acetonitrile (Burdick and Jackson). These samples were deoxygenated using the freeze–pump–thaw degassing method, repeating the process five times. The glass tubes were

then sealed under vacuum. On returning to room temperature, the samples were ready for lifetime measurements.

2.6. Electrochemistry

Cyclic voltammograms were obtained on a BioAnalytical Systems 100 W electrochemical analyzer. The solvent used was Burdick and Jackson acetonitrile dried over activated molecular sieves. The supporting electrolyte was tetrabutylammonium hexafluorophosphate (TBAH). Prior to each scan, the solutions were bubbled with argon for 20 min, and blanketed with argon during each scan. The three-electrode system used in the measurements consisted of a platinum auxiliary electrode, a platinum disk working electrode and an Ag/AgCl reference electrode (0.29 V vs. normal hydrogen electrode (NHE)).

2.7. Spectroelectrochemistry

In the spectroelectrochemical experiments performed in this study, the working electrode was a platinum mesh cylinder, the reference electrode was an Ag/AgCl gel electrode and the auxiliary electrode was a platinum mesh cylinder. The experiment was carried out in a cell designed and constructed in-house, which utilized a 1 cm quartz cuvette as the working compartment of an H cell [57]. The potential was controlled by a BAS 100 W electrochemical analyzer. The oxidative spectroelectrochemical experiment was carried out in 0.1 M NBu_4PF_6 acetonitrile solution, whereas reductive spectroelectrochemistry was performed in dimethylformamide solution to improve reversibility. The working compartment was deoxygenated by bubbling with argon prior to and during each experiment.

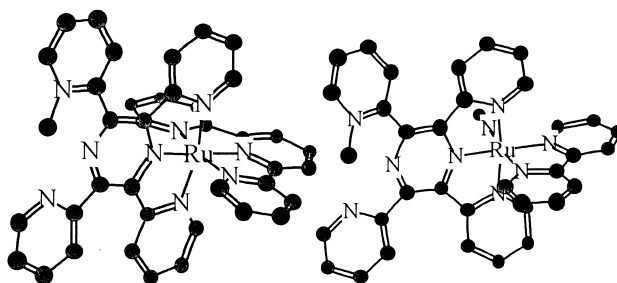
2.8. Nuclear magnetic resonance (NMR) spectroscopy

^1H and ^{13}C NMR measurements were made on saturated solutions in CD_3CN using a Varian Unity 400 MHz instrument.

3. Results and discussion

3.1. Synthesis

The preparation of the methylated complexes can be achieved in relatively high yield using simple synthetic methods [52]. Care must be taken to remove traces of unmethylated species from the final product. This is easily accomplished using adsorption chromatography on alumina.



3.2. NMR spectroscopy

The ^1H NMR spectra obtained on these methylated complexes are indicative of the proposed structure [52]. On methylation, a new ^1H resonance appears at 4.58 ppm for $[\text{Ru}(\text{tpy})(\text{Metpp})]^{3+}$ and 4.56 ppm for $[\text{Ru}(\text{bpy})(\text{Metpp})(\text{CH}_3\text{CN})]^{3+}$. Integration of this signal yields a ratio of 27 aromatic protons to three methyl protons for $[\text{Ru}(\text{tpy})(\text{Metpp})]^{3+}$ and 24 aromatic protons to three methyl protons for $[\text{Ru}(\text{bpy})(\text{Metpp})(\text{CH}_3\text{CN})]^{3+}$, consistent with the proposed structures possessing a singly methylated product. The ^1H NMR spectra show that methylation occurs at the pyridyl nitrogen as expected due to its greater nucleophilicity than that of the pyrazine nitrogen [52].

3.3. Electrochemistry

Predictions concerning the electrochemistry of these complexes can be made on the basis of previously studied ruthenium polyazine complexes [49,50,54,55]. The free ligand tpp is easier to reduce than either tpy or bpy, and will thus contain the acceptor or LUMO in mixed-ligand complexes of these ligands [49,50,54,55]. In ruthenium polypyridine complexes, the highest occupied molecular orbital (HOMO) is ruthenium based, with the metal oxidation potential being sensitive to the coordination environment of the ruthenium center [49,50,54,55].

Table 1 summarizes the cyclic voltammetric data for $[\text{Ru}(\text{tpy})(\text{tpp})]^{2+}$, $[\text{Ru}(\text{tpy})(\text{Metpp})]^{3+}$, $[\text{Ru}(\text{bpy})(\text{tpp})\text{Cl}]^+$, $[\text{Ru}(\text{bpy})(\text{tpp})(\text{CH}_3\text{CN})]^{2+}$ and $[\text{Ru}(\text{bpy})(\text{Metpp})(\text{CH}_3\text{CN})]^{3+}$. The electrochemistry of $[\text{Ru}(\text{tpy})(\text{tpp})]^{2+}$ has been reported previously [50,54,55], but

Table 1

Cyclic voltammetric data for a series of ruthenium(II) complexes involving the tridentate bridging ligand tpp (where bpy \equiv 2,2'-bipyridine, tpp \equiv 2,3,5,6-tetrakis(2-pyridyl)pyrazine, tpy \equiv 2,2':6',2''-terpyridine and Metpp \equiv 2-[2-(1-methylpyridinium)]-3,5,6-tris(2-pyridyl)pyrazine)

Compound	$E_{1/2}$ (V)	Assignment
$[\text{Ru}(\text{tpy})(\text{tpp})]^{2+}$	+1.40	Ru(II)/Ru(III)
	-0.97	tpp/tpp $^-$ (pyrazine)
	-1.38	tpy/tpy $^-$
	-1.60	tpp $^-$ /tpp $^{2-}$
$[\text{Ru}(\text{tpy})(\text{Metpp})]^{3+}$	+1.55	Ru(II)/Ru(III)
	-0.65	Metpp $^+$ /Metpp (viologen)
	-0.80	Metpp/Metpp $^-$ (pyrazine)
	-1.60	tpy/tpy $^-$
$[\text{Ru}(\text{bpy})(\text{tpp})\text{Cl}]^+$	+0.97	Ru(II)/Ru(III)
	-1.06	tpp/tpp $^-$ (pyrazine)
$[\text{Ru}(\text{bpy})(\text{tpp})(\text{CH}_3\text{CN})]^{2+}$	+1.36	Ru(II)/Ru(III)
	-0.97	tpp/tpp $^-$ (pyrazine)
	-1.48	bpy/bpy $^-$
$[\text{Ru}(\text{bpy})(\text{Metpp})(\text{CH}_3\text{CN})]^{3+}$	+1.54	Ru(II)/Ru(III)
	-0.51	Metpp $^+$ /Metpp (viologen)
	-0.72	Metpp/Metpp $^-$ (pyrazine)

Potentials reported vs. Ag/AgCl (0.29 V vs. NHE).

the potentials reported in Table 1 are those measured under our conditions to make comparisons more valid. In $[\text{Ru}(\text{tpy})(\text{tpp})]^{2+}$, the oxidation at +1.40 V has been assigned as a Ru(II)/Ru(III) metal-based process and the first reduction at -0.97 V is assigned as a tpp/tpp $^-$ -based reduction. We have shown previously using electron spin resonance (ESR) that Os complexes incorporating the tpp ligand exhibit a one-electron reduction which is localized on the pyrazine portion of the tpp ligand [49]. An analogous pyrazine-based reduction is expected for this $[\text{Ru}(\text{tpy})(\text{tpp})]^{2+}$ species. The second reduction in $[\text{Ru}(\text{tpy})(\text{tpp})]^{2+}$ at -1.38 V has been assigned as a tpy/tpy $^-$ ligand-centered process [50,54,55]. The third reduction at -1.60 V is assigned as a second tpp-based process (tpp $^-$ /tpp $^{2-}$) [49,50,54,55]. In $[\text{Ru}(\text{tpy})(\text{tpp})]^{2+}$, the HOMO is a ruthenium-based $d\pi$ orbital and the LUMO is a tpp ligand-based π^* orbital.

The methylated analog, $[\text{Ru}(\text{tpy})(\text{Metpp})]^{3+}$, exhibits a reversible Ru(II)/Ru(III) oxidation at +1.55 V and a series of reductions at -0.65, -0.80 and -1.46 V. On methylation, the ruthenium metal becomes harder to oxidize by 150 mV. This results from the addition of the viologen which increases the complex's positive charge and increases the Metpp ligand's π -accepting ability relative to tpp. A new reduction, more positive than the tpp/tpp $^-$ wave in $[\text{Ru}(\text{tpy})(\text{tpp})]^{2+}$, is observed for this methylated species at -0.65 V. This represents the reduction of the viologen moiety. The second reduction of $[\text{Ru}(\text{tpy})(\text{Metpp})]^{3+}$ is a reduction based on the pyrazine portion of the tpp ligand and occurs at a slightly more positive potential than that of the unmethylated analog, $[\text{Ru}(\text{tpy})(\text{tpp})]^{2+}$, consistent with the electron-withdrawing effect of the viologen substituent. The third reduction of $[\text{Ru}(\text{tpy})(\text{Metpp})]^{3+}$ at -1.46 V probably represents the reduction of the tpy ligand. In $[\text{Ru}(\text{tpy})(\text{Metpp})]^{3+}$, the HOMO is a ruthenium-based $d\pi$ orbital and the LUMO is a Metpp ligand-based orbital localized on the remote viologen portion of the ligand.

In the case of $[\text{Ru}(\text{bpy})(\text{tpp})\text{Cl}]^+$, the ruthenium oxidation occurs at +0.97 V and the tpp reduction at -1.06 V. A single reduction is reported since the complex becomes neutral after this process and adsorbs to the electrode surface. The shift of the ruthenium oxidation of $[\text{Ru}(\text{bpy})(\text{tpp})\text{Cl}]^+$ to a less positive potential relative to $[\text{Ru}(\text{tpy})(\text{tpp})]^{2+}$ is indicative of the π -donor nature of the chloride and the π -acceptor nature of tpy. This provides a more electron-rich metal in $[\text{Ru}(\text{bpy})(\text{tpp})\text{Cl}]^+$ which is substantially easier to oxidize. The tpp reduction shifts to a more negative potential in $[\text{Ru}(\text{bpy})(\text{tpp})\text{Cl}]^+$ relative to $[\text{Ru}(\text{tpy})(\text{tpp})]^{2+}$. This is the result of the more electron-rich Ru metal center having an increased π -backbonding interaction with the tpp ligand. This complex possesses an Ru($d\pi$) HOMO and a tpp(π^*) LUMO.

For $[\text{Ru}(\text{bpy})(\text{tpp})(\text{CH}_3\text{CN})]^{2+}$, the Ru(II)/Ru(III) oxidation occurs at +1.36 V, the tpp/tpp $^-$ reduction at -0.97 V and the bpy/bpy $^-$ reduction at -1.48 V. Substitution of the chloride ligand in $[\text{Ru}(\text{bpy})(\text{tpp})\text{Cl}]^+$ with an

acetonitrile to produce $[\text{Ru}(\text{bpy})(\text{tpp})(\text{CH}_3\text{CN})]^{2+}$ results in a complex which is harder to oxidize by 390 mV, consistent with the π -accepting ability of the coordinated acetonitrile ligand. The tpp reduction in the solvato complex occurs at a value 90 mV more positive than that of the chloride complex. This substitution of the chloride with acetonitrile leaves the ruthenium center less electron rich, decreasing the degree of π -backbonding to the tpp ligand and giving rise to the observed shift in the tpp-based reduction potential. This complex possesses an Ru($d\pi$) HOMO and a tpp(π^*) LUMO.

In comparing the methylated and unmethylated complexes $[\text{Ru}(\text{bpy})(\text{tpp})(\text{CH}_3\text{CN})]^{2+}$ and $[\text{Ru}(\text{bpy})(\text{Metpp})(\text{CH}_3\text{CN})]^{3+}$, we would expect to find results similar to those discussed above for $[\text{Ru}(\text{tpy})(\text{tpp})]^{2+}$ and $[\text{Ru}(\text{tpy})(\text{Metpp})]^{3+}$. On methylation, the ruthenium again becomes harder to oxidize: +1.54 V for $[\text{Ru}(\text{bpy})(\text{Metpp})(\text{CH}_3\text{CN})]^{3+}$ vs. +1.36 V for $[\text{Ru}(\text{bpy})(\text{tpp})(\text{CH}_3\text{CN})]^{2+}$. A new reductive process is observed at -0.51 V for the methylated complex and represents the reduction of the viologen portion of the tpp ligand. The second reduction of $[\text{Ru}(\text{bpy})(\text{Metpp})(\text{CH}_3\text{CN})]^{3+}$ represents the reduction of the pyrazine portion of the tpp ligand and occurs at -0.72 V. The reduction of the bpy ligand is not well resolved, presumably due to the formation of a neutral metal complex which adsorbs to the electrode surface. This $[\text{Ru}(\text{bpy})(\text{Metpp})(\text{CH}_3\text{CN})]^{3+}$ complex possesses an Ru($d\pi$) HOMO and a viologen-based LUMO.

The electrochemical studies indicate that all of the complexes prepared possess ruthenium ($d\pi$)-based HOMOs and the nature of the LUMO varies as a function of the structure. The unmethylated complexes $[\text{Ru}(\text{tpy})(\text{tpp})]^{2+}$ and $[\text{Ru}(\text{bpy})(\text{tpp})(\text{CH}_3\text{CN})]^{2+}$ possess LUMOs which are based on the pyrazine portion of the tpp ligand. Methylation to yield $[\text{Ru}(\text{tpy})(\text{Metpp})]^{3+}$ and $[\text{Ru}(\text{bpy})(\text{Metpp})(\text{CH}_3\text{CN})]^{3+}$ produces complexes in which the LUMO is based on the remote viologen portion of the Metpp ligand. This indicates that intramolecular electron transfer quenching of the Ru($d\pi$) \rightarrow tpp(π^*) charge transfer state is thermodynamically favored to produce a reduced viologen acceptor in the Metpp complexes. This is consistent with the molecular design.

3.4. Electronic absorption spectroscopy

The electronic absorption spectroscopy data are summarized in Table 2. The spectra for $[\text{Ru}(\text{tpy})(\text{tpp})]^{2+}$ and $[\text{Ru}(\text{tpy})(\text{Metpp})]^{3+}$ are shown in Fig. 1, whereas those for $[\text{Ru}(\text{bpy})(\text{tpp})\text{Cl}]^+$, $[\text{Ru}(\text{bpy})(\text{tpp})(\text{CH}_3\text{CN})]^{2+}$ and $[\text{Ru}(\text{bpy})(\text{Metpp})(\text{CH}_3\text{CN})]^{3+}$ are shown in Fig. 2. In metal complexes of these ligands, the UV region of the electronic absorption spectrum consists primarily of ligand-based $n \rightarrow \pi^*$ and $\pi \rightarrow \pi^*$ transitions. The visible region of the electronic absorption spectrum for polypyridyl ruthenium complexes contains bands which can be assigned as MLCT in nature terminating on each acceptor ligand [50,54,55].

Table 2

Photophysical data for a series of ruthenium(II) complexes containing the tridentate bridging ligand tpp (where bpy \equiv 2,2'-bipyridine, tpp \equiv 2,3,5,6-tetrakis(2-pyridyl)pyrazine, tpy \equiv 2,2':6',2''-terpyridine and Metpp \equiv 2-[2-(1-methylpyridinium)]-3,5,6-tris(2-pyridyl)pyrazine)

Compound	$\lambda_{\text{max}}^{\text{abs}}$ (nm) ^a	$\lambda_{\text{max}}^{\text{em}}$ (nm) ^b	τ (ns) ^b (Φ)
$[\text{Ru}(\text{tpy})(\text{tpp})]^{2+}$	474	665	30 (7.9×10^{-4})
$[\text{Ru}(\text{tpy})(\text{Metpp})]^{3+}$	474	700	38 (3.7×10^{-4})
$[\text{Ru}(\text{bpy})(\text{tpp})\text{Cl}]^+$	504	818	21
$[\text{Ru}(\text{bpy})(\text{tpp})(\text{CH}_3\text{CN})]^{2+}$	456	700	62 (6.8×10^{-4})
$[\text{Ru}(\text{bpy})(\text{Metpp})(\text{CH}_3\text{CN})]^{3+}$	458	712	70 (3.3×10^{-4})

^a Measured in CH_3CN at room temperature.

^b Measured in deoxygenated CH_3CN at room temperature.

A comparison of the electronic absorption spectra of the two sets of complexes reveals some interesting features. These spectra are virtually identical for the Metpp and tpp analogs, despite the very different electrochemistry. This indicates that, although the viologen LUMO has been added in the Metpp system, this viologen orbital is localized on the remote ring system and thus does not display significant overlap with the metal-based orbitals. Therefore the introduction of the viologen does not perturb the light-absorbing properties of the Ru^{II}(tpy)(tpp) moiety and no Ru \rightarrow viologen charge transfer band appears in the electronic absorption spectrum. The lowest energy transition for both $[\text{Ru}(\text{tpy})(\text{tpp})]^{2+}$ and $[\text{Ru}(\text{tpy})(\text{Metpp})]^{3+}$ is at 474 nm. The energy of this transition remains the same on methylation, indicating that the acceptor orbital for this transition for both the methylated and unmethylated complexes is the same, i.e. the pyrazine portion of the tpp ligand. This lowest energy absorption has a high-energy shoulder attributed to the Ru($d\pi$) \rightarrow tpy(π^*) MLCT transition [50,54,55]. An Ru($d\pi$) \rightarrow viologen charge transfer transition is not observed, presumably due to a lack of sufficient orbital overlap as a result of the localization of this viologen orbital on the remote ring. Both the methylated and unmethylated complexes possess the same lowest lying spectroscopically accessible excited state which is Ru \rightarrow tpp charge transfer in nature.

The electronic absorption spectra of the bpy-containing complexes show some interesting trends. The spectra are shown in Fig. 2. $[\text{Ru}(\text{bpy})(\text{tpp})\text{Cl}]^+$ has a lowest lying absorbance at 504 nm which is assigned as an Ru($d\pi$) \rightarrow tpp(π^*) charge transfer transition. The MLCT transition is shifted to higher energy, 456 nm, on substitution of the chloride with acetonitrile to produce $[\text{Ru}(\text{bpy})(\text{tpp})(\text{CH}_3\text{CN})]^{2+}$. This is consistent with the electrochemical results, which indicate that the ruthenium $d\pi$ orbitals are stabilized on substitution of the chloride by acetonitrile. The $[\text{Ru}(\text{bpy})(\text{tpp})\text{Cl}]^+$ complex is also expected to possess an intense Ru($d\pi$) \rightarrow bpy(π^*) charge transfer band. This peak is probably contained within the broad peak at 504 nm, and will be higher in energy relative to the Ru($d\pi$) \rightarrow tpp(π^*) charge transfer transition.

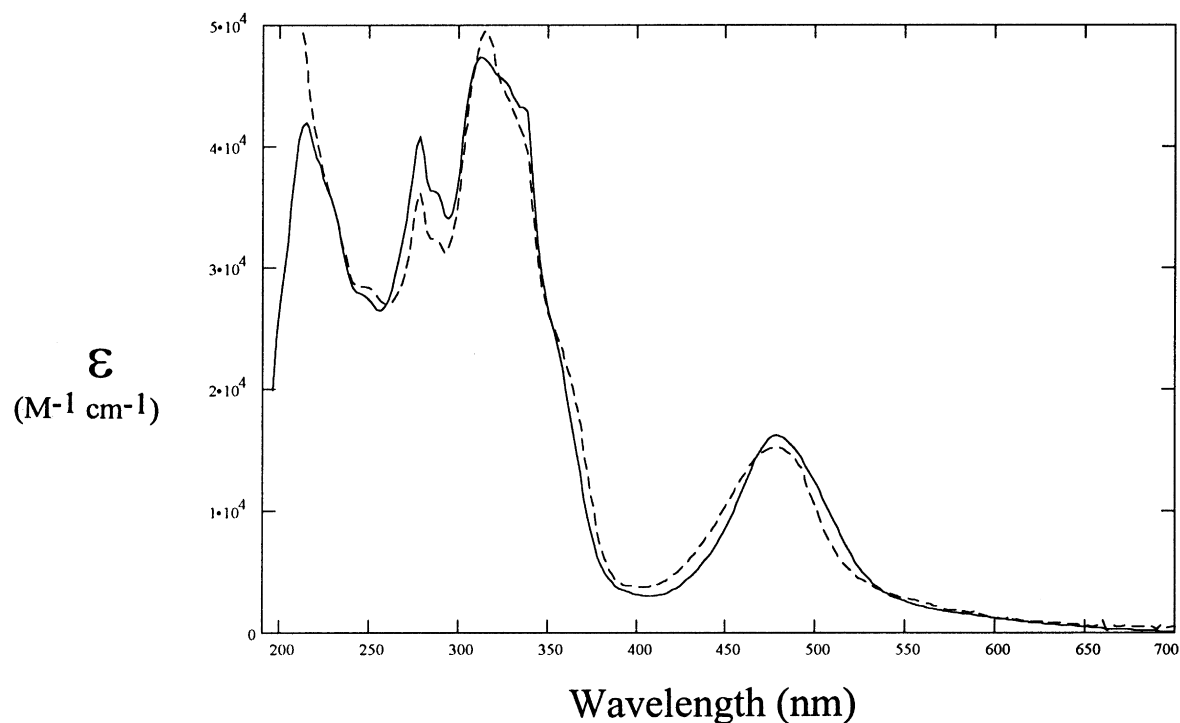


Fig. 1. Electronic absorption spectra (acetonitrile solutions) for $[\text{Ru}(\text{tpy})(\text{tpp})]^{2+}$ (—) and $[\text{Ru}(\text{tpy})(\text{Metpp})]^{3+}$ (---) (where tpy \equiv 2,2':6',2''-terpyridine, tpp \equiv 2,3,5,6-tetrakis(2-pyridyl)pyrazine and Metpp \equiv 2-[2-(1-methylpyridinium)]-3,5,6-tris(2-pyridyl)pyrazine).

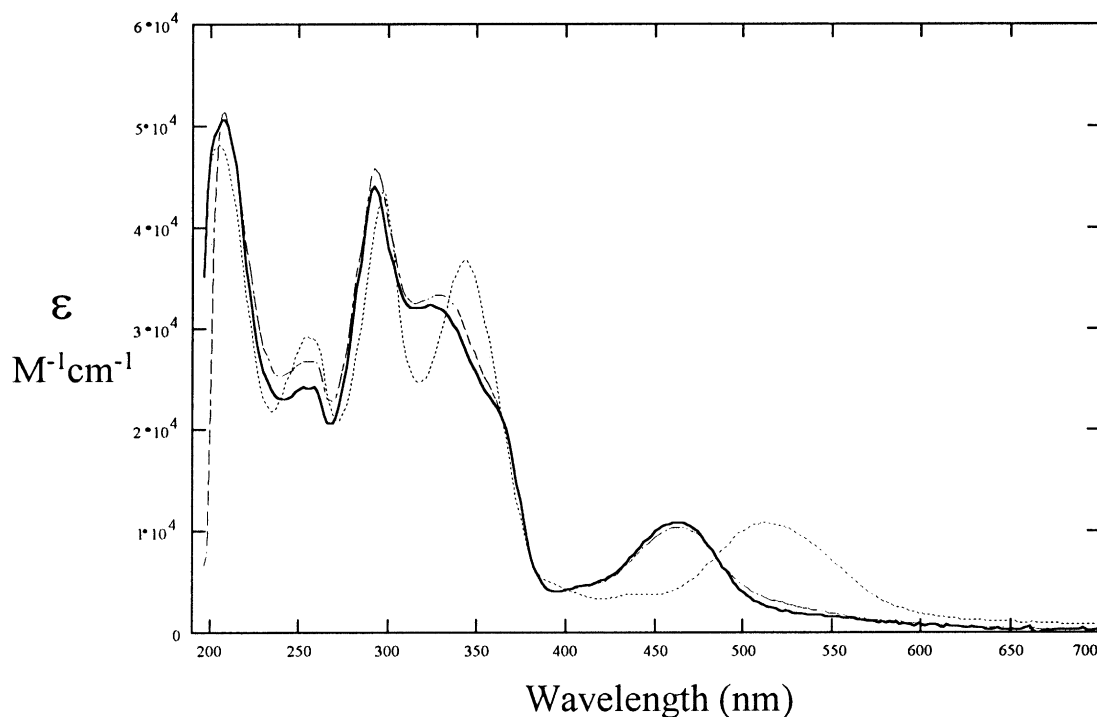


Fig. 2. Electronic absorption spectra (acetonitrile solutions) for $[\text{Ru}(\text{bpy})(\text{tpp})\text{Cl}]^+$ (\cdots), $[\text{Ru}(\text{bpy})(\text{tpp})(\text{CH}_3\text{CN})]^{2+}$ (—) and $[\text{Ru}(\text{bpy})(\text{Metpp})(\text{CH}_3\text{CN})]^{3+}$ (---) (where bpy \equiv 2,2'-bipyridine, tpp \equiv 2,3,5,6-tetrakis(2-pyridyl)pyrazine and Metpp \equiv 2-[2-(1-methylpyridinium)]-3,5,6-tris(2-pyridyl)pyrazine).

A comparison of the electronic absorption spectra of $[\text{Ru}(\text{bpy})(\text{tpp})(\text{CH}_3\text{CN})]^{2+}$ and $[\text{Ru}(\text{bpy})(\text{Metpp})(\text{CH}_3\text{CN})]^{3+}$ in Fig. 2 shows some interesting features. Once again, the spectra of the methylated $[\text{Ru}(\text{bpy})(\text{Metpp})(\text{CH}_3\text{CN})]^{3+}$ and unmethylated $[\text{Ru}(\text{bpy})-$

$(\text{tpp})(\text{CH}_3\text{CN})]^{2+}$ complexes are virtually identical. This illustrates that, in this framework, the viologen orbital is localized on the remote ring and the addition of the viologen does not perturb the spectroscopic properties of the $\text{Ru}^{\text{II}}(\text{bpy})(\text{tpp})(\text{CH}_3\text{CN})$ chromophore. The lowest energy

transition at 456 nm for $[\text{Ru}(\text{bpy})(\text{tpp})(\text{CH}_3\text{CN})]^{2+}$ and $[\text{Ru}(\text{bpy})(\text{Metpp})(\text{CH}_3\text{CN})]^{3+}$ corresponds to an $\text{Ru}(\text{d}\pi) \rightarrow \text{tpp}(\pi^*)$ charge transfer terminating on the pyrazine portion of the tpp ligand. These complexes also possess very broad bands in this region, indicative of the overlapping nature of the $\text{Ru} \rightarrow \text{tpp}$ and $\text{Ru} \rightarrow \text{bpy}$ charge transfer transitions. Again the $\text{Ru} \rightarrow \text{tpp}$ charge transfer component will occur at lower energy. As in the $[\text{Ru}(\text{tpy})(\text{Metpp})]^{3+}$ system, this $[\text{Ru}(\text{bpy})(\text{Metpp})(\text{CH}_3\text{CN})]^{3+}$ complex does not display an $\text{Ru} \rightarrow \text{viologen}$ charge transfer absorbance due to the lack of sufficient orbital overlap.

Both sets of methylated and unmethylated analogs possess the same lowest lying spectroscopically accessible excited state, $\text{Ru}(\text{d}\pi) \rightarrow \text{tpp}(\pi^*)$ charge transfer. This result, coupled with the electrochemical analysis described above, indicates that optical population of this MLCT state will occur and can be followed by intramolecular electron transfer for the Metpp systems to produce a reduced viologen and an oxidized ruthenium.

3.5. Spectroelectrochemistry

Spectroelectrochemistry was used to correlate the spectroscopy and electrochemistry of these systems. In the spectroelectrochemical experiments performed in this study, the complex was either oxidized or reduced at a potential corresponding to a one-electron process. Monitoring this by electronic absorption spectroscopy aids in the interpretation of the spectroscopy and electrochemistry of the complexes.

When the free ligand tpp is reduced to -1.70 V, new $\pi^* \rightarrow \pi^*$ transitions appear in the visible at 425 and 530 nm [58]. In the spectroelectrochemical results for the complexes incorporating tpp, this will be expected to obscure changes anticipated for the MLCT transitions in this region on tpp reduction.

Fig. 3(a) shows the results for the oxidative spectroelectrochemistry of $[\text{Ru}(\text{tpy})(\text{tpp})]^{2+}$ [50]. Electrogeneration of the oxidized complexes is possible with more than 95% regeneration of the original oxidation state. As predicted, the $\text{Ru} \rightarrow \text{tpy}$ and $\text{Ru} \rightarrow \text{tpp}$ charge transfer transitions at 474 nm are lost on one-electron oxidation of the ruthenium metal, consistent with these being transitions involving the metal center. The peaks at 330 and 360 nm appear to shift to lower energy on metal oxidation, consistent with a ligand-based $\pi \rightarrow \pi^*$ assignment. The lowest energy $\pi \rightarrow \pi^*$ transition at 360 nm should represent a tpp-based transition, whereas the band at 330 nm probably represents a tpy-based $\pi \rightarrow \pi^*$ transition. The peak at 310 nm is lost on metal oxidation, consistent with a higher energy MLCT band.

In Fig. 3(b), the reductive spectroelectrochemistry of $[\text{Ru}(\text{tpy})(\text{tpp})]^{2+}$ is shown [50]. The regeneration of the original oxidation state from the one-electron-reduced species is reversible to approximately 80%. As expected, the peak at 360 nm is lost on reduction of the tpp ligand. This confirms our assignment of this peak as a tpp-based $\pi \rightarrow \pi^*$ transition. The peaks at 310 and 330 nm remain on tpp reduc-

tion. This is consistent with a higher energy $\text{Ru} \rightarrow \text{tpy}$ charge transfer band at 310 nm and a tpy $\pi \rightarrow \pi^*$ band at 330 nm. Some intensity is lost in the 450–500 nm region when the tpp ligand is reduced, consistent with a loss of the $\text{Ru} \rightarrow \text{tpp}$ charge transfer band in this region. Peaks appear in the 400–500 nm region and probably represent tpp-based $\pi^* \rightarrow \pi^*$ bands. A new peak at approximately 680 nm in the reduced species may represent a tpp $\rightarrow \text{Ru}$ ligand-to-metal charge transfer (LMCT) band. This spectrum of the one-electron-reduced form of $[\text{Ru}(\text{tpy})(\text{tpp})]^{2+}$ can be used for comparison with the Metpp analog to ensure that the first reduction in $[\text{Ru}(\text{tpy})(\text{Metpp})]^{3+}$ is not localized on the same orbital as that of the tpp system, but is in fact viologen based.

Fig. 4 shows the results for the spectroelectrochemistry of $[\text{Ru}(\text{tpy})(\text{Metpp})]^{3+}$. Electrogeneration of the oxidized complex is possible, with more than 95% regeneration of the original oxidation state. As expected, the oxidation of ruthenium results in a similar spectrum as that of the unmethylated complex, $[\text{Ru}(\text{tpy})(\text{tpp})]^{2+}$. The band at 474 nm, which has been assigned as overlapping $\text{Ru} \rightarrow \text{tpy}$ and $\text{Ru} \rightarrow \text{tpp}$ MLCT transitions, is lost on metal oxidation. In Fig. 4(b), the absorption spectra are shown for $[\text{Ru}(\text{tpy})(\text{Metpp})]^{3+}$ and its one-electron-reduced form. Electrogeneration of the one-electron-reduced species is reversible, with more than 95% regeneration of the original oxidation state. It has been noted by Jones et al. [59] that the one-electron reduction of MQ^+ (where $\text{MQ}^+ \equiv N\text{-methyl-4,4'-bipyridinium cation}$) results in a visible absorption spectrum containing a band at 535 nm. This corresponds to reduction of the viologen portion of this ligand. In metal complexes incorporating this ligand, increases in absorbance on reduction of the viologen occur at 358, 480 and 595 nm [59]. A similar behavior would be expected on one-electron reduction of $[\text{Ru}(\text{tpy})(\text{Metpp})]^{3+}$, since the first reduction is assigned to reduction of the viologen portion of the Metpp ligand. One-electron reduction of this complex results in increases in absorbance throughout the visible, with new peaks appearing at 360, 480 and 600 nm. This result is inconsistent with the reduction of the pyrazine portion of tpp as in the complex $[\text{Ru}(\text{tpy})(\text{tpp})]^{2+}$ and consistent with a viologen-based reduction [50,59]. This further confirms the assignment of the first reduction in this complex as being viologen based.

3.6. Emission spectroscopy and excited state lifetimes

All the complexes reported emit in solution at room temperature in marked contrast with the well-studied $[\text{Ru}(\text{tpy})_2]^{2+}$ [60]. The presence of observable emission in our systems results from the lower energy of the $\text{tpp}(\pi^*)$ acceptor orbital relative to tpy [50,51]. This gives rise to a stabilized MLCT state which limits thermal population of the ligand field (LF) state at room temperature. It is this LF state which is responsible for the lack of emission at room temperature for $[\text{Ru}(\text{tpy})_2]^{2+}$ [60]. The photophysical data for $[\text{Ru}(\text{tpy})(\text{tpp})]^{2+}$, $[\text{Ru}(\text{tpy})(\text{Metpp})]^{3+}$, $[\text{Ru}(\text{bpy})-$

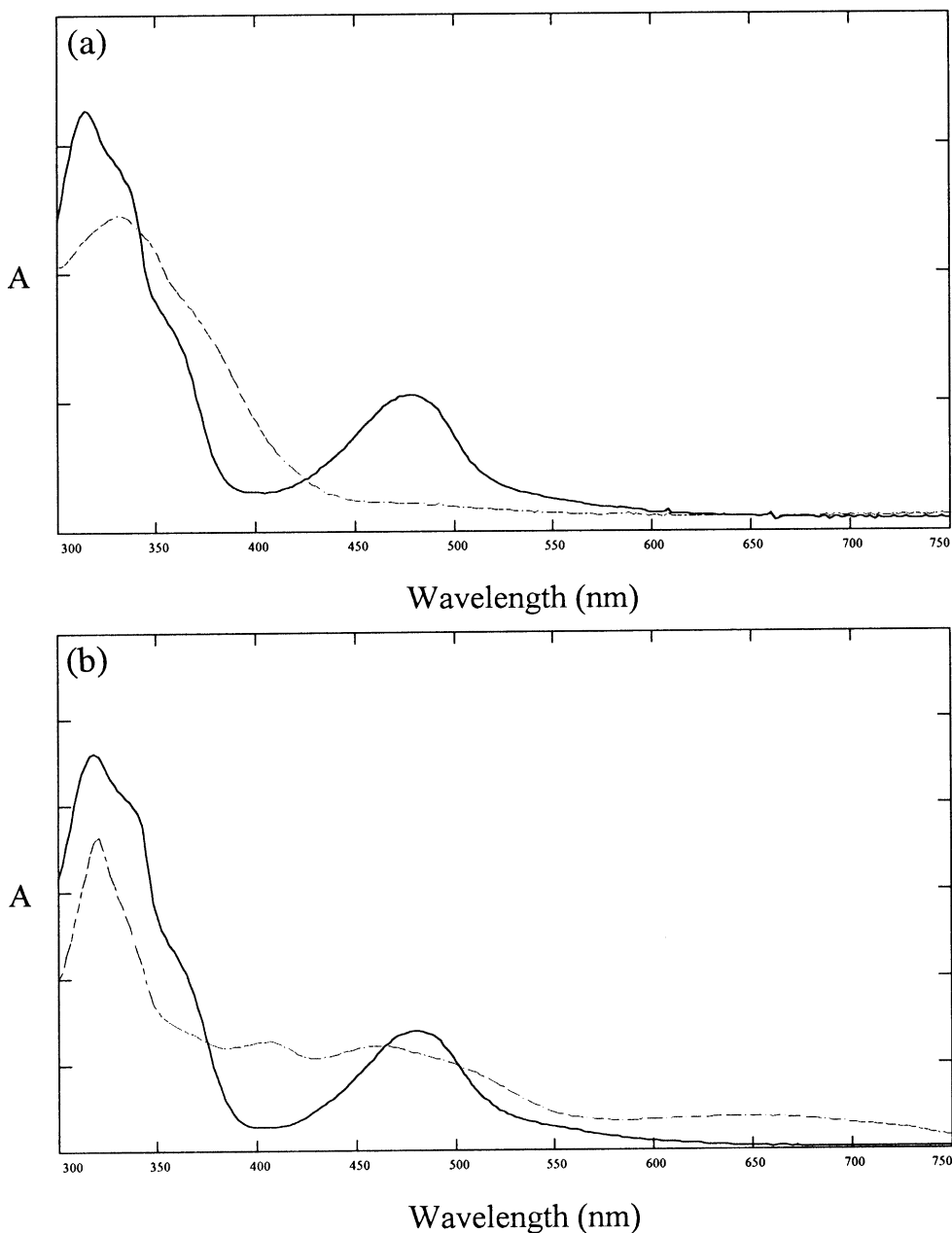


Fig. 3. Spectroelectrochemical results for $[\text{Ru}(\text{tpy})(\text{tpp})]^{2+}$ (where $\text{tpy} \equiv 2,2':6',2''$ -terpyridine and $\text{tpp} \equiv 2,3,5,6$ -tetrakis(2-pyridyl)pyrazine): (a) original oxidation state (—) and one-electron oxidation (---); (b) original oxidation state (—) and one-electron reduction (---).

$(\text{tpp})\text{Cl}]^+$, $[\text{Ru}(\text{bpy})(\text{tpp})(\text{CH}_3\text{CN})]^{2+}$ and $[\text{Ru}(\text{bpy})-(\text{Metpp})(\text{CH}_3\text{CN})]^{3+}$ are summarized in Table 2. For polypyridyl complexes of this type, we expect to observe emission from the lowest lying $^3\text{MLCT}$ excited state. This emission will occur at a lower energy than absorption, since absorption involves a $^1\text{MLCT}$ transition, whereas the emission arises from a $^3\text{MLCT}$ state.

In agreement with absorption spectroscopy, substitution of the coordinated chloride in $[\text{Ru}(\text{bpy})(\text{tpp})\text{Cl}]^+$ by an acetonitrile solvent molecule to form $[\text{Ru}(\text{bpy})(\text{tpp})(\text{CH}_3\text{CN})]^{2+}$ leads to a higher energy emission. When comparing the methylated and unmethylated systems, slight shifts in the emission maxima to lower energy occur on methyla-

tion. The emission spectrum of $[\text{Ru}(\text{tpy})(\text{tpp})]^{2+}$ has been published previously [49,50,54,55]. $[\text{Ru}(\text{tpy})(\text{tpp})]^{2+}$ emits at 665 nm, whereas $[\text{Ru}(\text{tpy})(\text{Metpp})]^{3+}$ emits at 700 nm. Similar results are found in $[\text{Ru}(\text{bpy})(\text{tpp})(\text{CH}_3\text{CN})]^{2+}$ and $[\text{Ru}(\text{bpy})(\text{Metpp})(\text{CH}_3\text{CN})]^{3+}$, where the emission occurs at 700 nm and 712 nm respectively. All of the complexes studied emit from the $\text{Ru}(d\pi) \rightarrow \text{tpp}(\pi^*)$ $^3\text{MLCT}$ excited state in which the acceptor orbital is localized on the pyrazine portion of the ligand. The slightly lower energy emission of the Metpp complexes results from the stabilization of the pyrazine-based orbital by the introduction of the electron-withdrawing viologen substituent. This is shown in the Jablonski diagrams in Fig. 5.

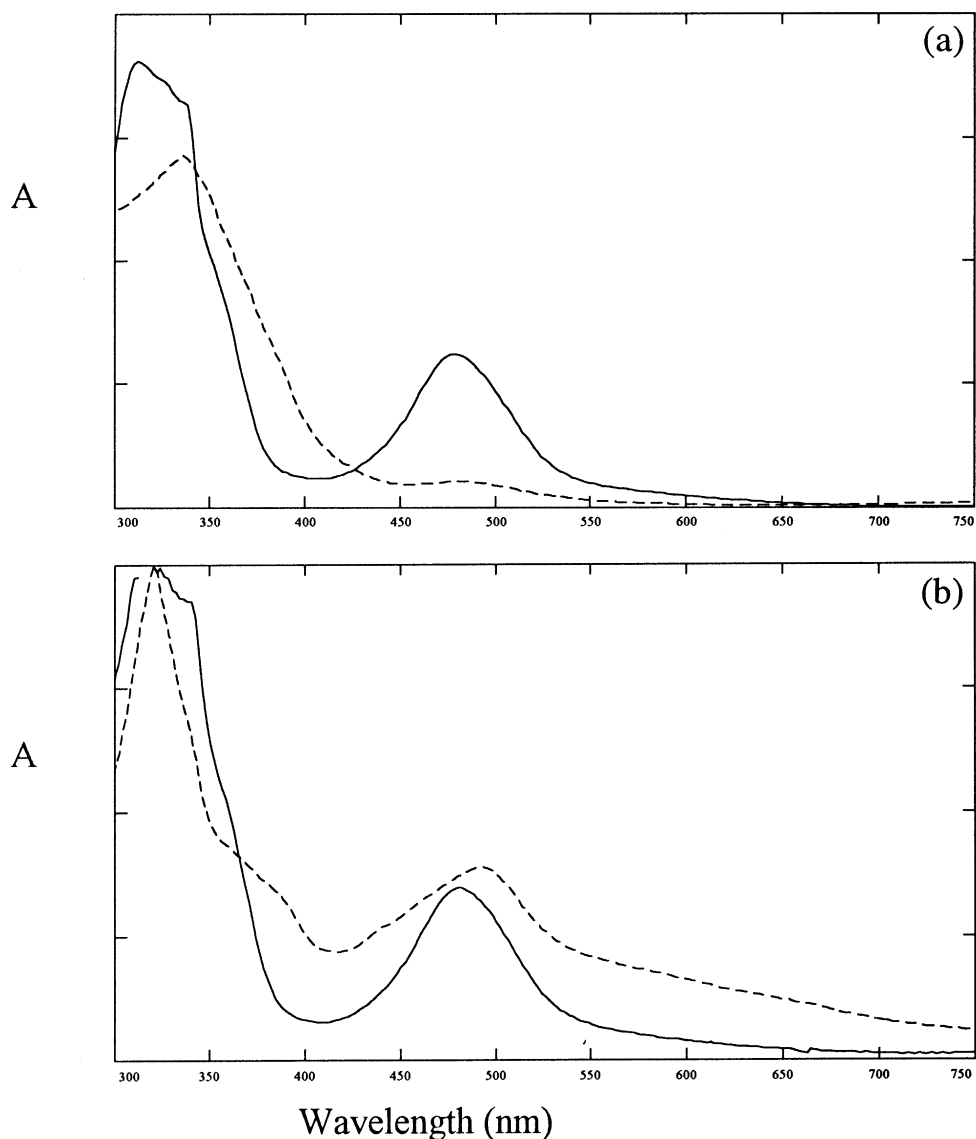


Fig. 4. Spectroelectrochemical results for $[\text{Ru}(\text{tpy})(\text{Metpp})]^{3+}$ (where $\text{tpy} \equiv 2,2':6',2''\text{-terpyridine}$ and $\text{Metpp} \equiv 2\text{-}[2\text{-}(1\text{-methylpyridinium})]\text{-}3,5,6\text{-tris}(2\text{-pyridyl})\text{pyrazine}$): (a) original oxidation state (—) and one-electron oxidation (---); (b) original oxidation state (—) and one-electron reduction (---).

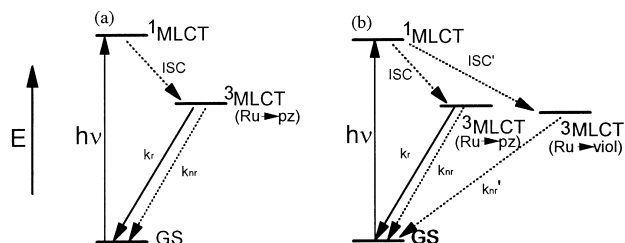


Fig. 5. Jablonski diagrams for $[\text{Ru}(\text{tpy})(\text{tpp})]^{2+}$ (a) and $[\text{Ru}(\text{tpy})(\text{Metpp})]^{3+}$ (b) (where $\text{tpy} \equiv 2,2':6',2''\text{-terpyridine}$, $\text{tpp} \equiv 2,3,5,6\text{-tetrakis}(2\text{-pyridyl})\text{pyrazine}$ and $\text{Metpp} \equiv 2\text{-}[2\text{-}(1\text{-methylpyridinium})]\text{-}3,5,6\text{-tris}(2\text{-pyridyl})\text{pyrazine}$).

Analysis of the 77 K emission of these complexes shows very similar vibronic structure for all of the systems: approximately 1200 cm^{-1} for $[\text{Ru}(\text{tpy})(\text{tpp})]^{2+}$, $[\text{Ru}(\text{tpy})(\text{Metpp})]^{3+}$, $[\text{Ru}(\text{bpy})(\text{tpp})(\text{CH}_3\text{CN})]^{2+}$ and $[\text{Ru}(\text{bpy})(\text{Metpp})(\text{CH}_3\text{CN})]^{3+}$. This corresponds to the

C–C and C–N pyridine-based ring modes typical of MLCT excited states of similar complexes [1,2]. This similarity in vibronic structure indicates that the same states are involved in the emission bands of the two sets of methylated and unmethylated complexes.

Based on the electrochemical studies, we would expect to see intramolecular electron transfer quenching of the $^3\text{MLCT}$ excited state localized on the pyrazine (pz) ring in systems containing the Metpp ligand. This would generate a charge-separated state with a reduced viologen and oxidized ruthenium. This intramolecular electron transfer should quench the emission of the $^3\text{MLCT}$ state in the Metpp systems.

The excited state lifetimes for each set of Metpp and tpp analogs are identical within the resolution of our measurements: 30–40 ns for the $[\text{Ru}(\text{tpy})(\text{tpp})]^{2+}$ and $[\text{Ru}(\text{tpy})(\text{Metpp})]^{3+}$ series and 60–70 ns for the $[\text{Ru}$

(bpy)(tpp)(CH₃CN)]²⁺ and [Ru(bpy)(Metpp)(CH₃CN)]³⁺ series. The emission quantum yields of the Metpp complexes are about half the values of the tpp analogs. Since both the Metpp and tpp systems have the same emissive state, relatively similar values of the rate constants for radiative (k_r) and non-radiative (k_{nr}) decay are expected in each set of tpp and Metpp analogs. If the quenching of the emission of the ³MLCT (Ru → pz) excited state occurs by electron transfer from this state, assuming equivalent values of k_r and k_{nr} for the tpp and Metpp analogs, we would expect the ratio of the quantum yields of emission for the tpp and Metpp analogs to be equal to the ratio of the excited state lifetimes of these states, i.e. $\Phi_{tpp}/\Phi_{Metpp} = \tau_{tpp}/\tau_{Metpp}$. This is clearly not the case. The decrease in Φ^{em} in the Metpp complexes, while maintaining a constant τ , leads to two possible conclusions. One explanation could be that the tpp and Metpp analogs have different values of k_r . This seems unlikely given the very similar emissive states in these sets of complexes. An alternative explanation could be that the optically populated ¹MLCT (Ru → pz) state undergoes intersystem crossing to both the emissive ³MLCT (Ru → pz) state as well as the charge-separated ³MLCT (Ru → viologen) state. This partitioning of the ¹MLCT state into two ³MLCT states would lead to an observed decrease in the quantum yield of emission of the Metpp systems, while still maintaining the same lifetime of the emissive ³MLCT (Ru → pz) state once populated. This seems to be the more plausible explanation for the observed emission quantum yields and lifetimes, and is displayed in the Jablonski diagram in Fig. 5.

4. Conclusions

The preparation of a series of ruthenium complexes containing a covalently attached electron acceptor has been accomplished via methylation of the remote nitrogen on the tpp ligand. The electrochemistry of the Metpp complexes shows a viologen-based reduction followed by the traditional pyrazine-based process. These Metpp systems contain a viologen-based LUMO. The electronic absorption spectra of the methylated species are the same as those of the unmethylated analogs. The lowest energy transition is assigned as an Ru(dπ) → tpp(π*) charge transfer transition localized on the pyrazine ring of the tpp ligand. This excited state is emissive in fluid solution at room temperature. Quenching of the emission quantum yield in the methylated systems, with maintenance of the excited state lifetime of the emissive state, is observed in both sets of complexes. This probably results from a partitioning of the optically populated ¹MLCT state into both the emissive ³MLCT (Ru → pz) and charge-separated ³MLCT (Ru → viologen) states. Further investigation into these types of complexes is warranted. Larger polymetallic complexes can be constructed which incorporate the Metpp ligand by substitution of the remote tpy or bpy with a polyazine bridging ligand. By synthesizing larger, multimetallic complexes with more remote oxidizable moieties, the

charge separation distance will be increased. The presence of the coordinated acetonitrile ligand in [Ru(bpy)(Metpp)(CH₃CN)]³⁺ also facilitates synthetic modification of these systems.

Acknowledgements

Special thanks are due to Tom Glass for obtaining the NMR spectra. The authors wish to thank a reviewer for useful comments concerning the interpretation of the photophysical data of the complexes. This investigation was supported in part by funds provided by the National Science Foundation (CHE-9313642) and the Exxon Education Foundation. We also wish to thank Johnson Matthey for the generous loan of ruthenium trichloride used in this study.

References

- [1] A. Juris, V. Balzani, E. Barigelli, S. Campagna, P. Belser, *Coord. Chem. Rev.* 84 (1988) 85.
- [2] K. Kalyanasundaram, *Coord. Chem. Rev.* 46 (1982) 159.
- [3] J.N. Demas, A.W.J. Adamson, *J. Am. Chem. Soc.* 93 (1972) 1800.
- [4] H.D. Gafney, A.W. Adamson, *J. Am. Chem. Soc.* 94 (1972) 8238.
- [5] G. Navon, N. Sutin, *Inorg. Chem.* 13 (1974) 2159.
- [6] C.R. Bock, T.J. Meyer, D.G. Whitten, *J. Am. Chem. Soc.* 96 (1974) 4710.
- [7] C.T. Lin, W. Bottcher, M. Chou, C. Creutz, N. Sutin, *J. Am. Chem. Soc.* 98 (1976) 6536.
- [8] N.A.P. Kane-Maguire, C.H. Langford, *J. Am. Chem. Soc.* 94 (1972) 2121.
- [9] N. Sabbatini, V. Balzani, *J. Am. Chem. Soc.* 94 (1972) 7587.
- [10] T.J. Meyer, *Acc. Chem. Res.* 11 (1978) 94.
- [11] N. Sutin, C. Creutz, *Adv. Chem. Ser.* 168 (1978) 1.
- [12] J.P. Sauvage, J.P. Collin, J.C. Chambion, S. Guillerez, C. Coudret, V. Balzani, F. Barigelli, L. DeCola, L. Flamigni, *Chem. Rev.* 94 (1994) 995.
- [13] E. Danielson, C.M. Elliott, J.W. Merkert, T.J. Meyer, *J. Am. Chem. Soc.* 109 (1987) 2519.
- [14] J.P. Collin, S. Guillerez, J.P. Sauvage, F. Barigelli, L. DeCola, L. Flamigni, V. Balzani, *Inorg. Chem.* 31 (1992) 4112.
- [15] J.P. Collin, S. Guillerez, J.P. Sauvage, *J. Chem. Soc., Chem. Commun.* (1989) 776.
- [16] J.P. Collin, S. Guillerez, J.P. Sauvage, F. Barigelli, L. DeCola, L. Flamigni, V. Balzani, *Inorg. Chem.* 30 (1991) 4230.
- [17] J.-P. Collin, A. Harriman, V. Heitz, F. Odobel, J.-P. Sauvage, *J. Am. Chem. Soc.* 116 (1994) 5679.
- [18] A. Harriman, F. Odobel, J.-P. Sauvage, *J. Am. Chem. Soc.* 116 (1994) 5481.
- [19] F. Barigelli, L. Flamigni, V. Balzani, J.-P. Collin, J.-P. Sauvage, A. Sour, E.C. Constable, A. Thompson, *J. Am. Chem. Soc.* 116 (1994) 7692.
- [20] M.T. Indelli, C.A. Bignozzi, A. Harriman, J.R. Schoonover, F. Scandola, *J. Am. Chem. Soc.* 116 (1994) 3768.
- [21] G.F. Strouse, J.R. Schoonover, R. Duesing, T.J. Meyer, *Inorg. Chem.* 34 (1995) 2725.
- [22] P. Chen, D. Westmoreland, E. Danielson, K.S. Scahnze, D. Anthon, P.E. Nevez, T.J. Meyer, *Inorg. Chem.* 26 (1987) 1116.
- [23] K.A. Opperman, S.L. Mecklenburg, T.J. Meyer, *Inorg. Chem.* 33 (1994) 5295.
- [24] R. Duesing, G. Tapolsky, T.J. Meyer, *J. Am. Chem. Soc.* 112 (1990) 5378.

- [25] C.K. Ryu, R. Wang, R.H. Schmehl, S. Ferrere, M. Ludwikow, J.W. Merkert, C.E. Headford, C.M. Elliott, *J. Am. Chem. Soc.* 114 (1992) 430.
- [26] Y. Wang, K.S. Schanze, *J. Phys. Chem.* 99 (1995) 6876.
- [27] Y. Wang, B.T. Hauser, M.M. Rooney, R.D. Burton, K.S. Schanze, *J. Am. Chem. Soc.* 115 (1993) 5675.
- [28] Y. Wang, K.S. Schanze, *Chem. Phys.* 176 (1993) 305.
- [29] D. Gust, T.A. Moore, A.L. Moore, A.N. Macpherson, A. Lopez, J.M. DeGraziano, I. Garni, E. Bittersmann, G.R. Seely, F. Gao, R.A. Nieman, X.C. Ma, L.J. Demanche, S.-C. Hung, D.K. Luttrull, S.-J. Lee, P.K. Kerrigan, *J. Am. Chem. Soc.* 115 (1993) 11 141.
- [30] D. Gust, T.A. Moore, A.L. Moore, S.-J. Lee, E.B. Bittersmann, D.K. Luttrull, A.A. Rehms, J.M. DeGraziano, X.C. Ma, F. Gao, R.E. Belford, T.T. Tries, *Science* 248 (1990) 199.
- [31] A.N. Macpherson, P.A. Liddel, S. Lin, L. Noss, G.R. Seely, J.M. DeGraziano, A.L. Moore, T.A. Moore, D. Gust, *J. Am. Chem. Soc.* 117 (1995) 7202.
- [32] D. Gust, T.A. Moore, A.L. Moore, *Alternative Fuels and the Environment*, Lewis Publishers, 1995, p. 125.
- [33] S.-J. Lee, J.M. DeGraziano, A.N. Macpherson, E.-J. Shin, P.K. Kerrigan, G.R. Seely, A.L. Moore, T.A. Moore, D. Gust, *Chem. Phys.* 176 (1993) 321.
- [34] J.R. Schoonover, P. Chen, W.D. Bates, R.B. Dyer, T.J. Meyer, *Inorg. Chem.* 32 (1993) 1167.
- [35] Y. Fuchs, S. Lofters, T. Dieter, W. Shi, R. Morgan, T.C. Streckas, H.D. Gafney, A.D. Baker, *J. Am. Chem. Soc.* 109 (1987) 2691.
- [36] D.P. Rillema, K.B. Mack, *Inorg. Chem.* 21 (1982) 3849.
- [37] J.B. Cooper, D.B. MacQueen, J.D. Petersen, D.W. Wertz, *Inorg. Chem.* 29 (1990) 3901.
- [38] R.R. Ruminski, J.D. Petersen, *Inorg. Chem.* 21 (1982) 3706.
- [39] W.R. Murphy, K.J. Brewer, G. Gettliffe, J.D. Petersen, *Inorg. Chem.* 28 (1989) 81.
- [40] J.A. Baiano, D.L. Carlson, G.M. Wolosh, D.E. DeJesus, C.F. Knowles, E.G. Szabo, W.R. Murphy, *Inorg. Chem.* 29 (1990) 2327.
- [41] G. Tapolsky, R. Duesing, T.J. Meyer, *Inorg. Chem.* 29 (1990) 2285.
- [42] G. Denti, S. Campagna, L. Sabatino, S. Scolastica, M. Ciano, V. Balzani, *Inorg. Chem.* 29 (1990) 4750.
- [43] S. Campagna, G. Denti, S. Serroni, M. Ciano, A. Juris, B. Balzani, *Inorg. Chem.* 31 (1992) 2982.
- [44] L. DeCola, V. Balzani, F. Barigelletti, L. Flamigni, P. Belser, A. von Zelewsky, M. Frank, F. Vogtle, *Inorg. Chem.* 32 (1993) 5228.
- [45] S. Serroni, A. Juris, S. Campagna, M. Venturi, G. Denti, V. Balzani, *J. Am. Chem. Soc.* 116 (1994) 9086.
- [46] G. Giuffrida, S. Campagna, *Coord. Chem. Rev.* 135 (1994) 517.
- [47] G.F. Strouse, J.R. Schoonover, R. Duesing, S. Boyde, W.E. Jones, T.J. Meyer, *Inorg. Chem.* 34 (1995) 473.
- [48] M.M. Richter, K.J. Brewer, *Inorg. Chem.* 32 (1993) 7827; 31 (1992) 1594; 32 (1993) 5762. S.M. Molnar, G.E. Jensen, L.M. Vogler, S.W. Jones, L. Laverman, J.S. Bridgewater, M.M. Richter, K.J. Brewer, *J. Photochem. Photobiol. A: Chem.* 80 (1994) 315. S.M. Molnar, J.S. Bridgewater, G.N. Nallas, K.J. Brewer, *J. Am. Chem. Soc.* 116 (1994) 5206. M. Milkevitch, E. Brauns, K.J. Brewer, *Inorg. Chem.* 35 (1996) 1737.
- [49] R.G. Brewer, G.E. Jensen, K.J. Brewer, *Inorg. Chem.* 33 (1994) 124.
- [50] L.M. Vogler, B. Scott, K.J. Brewer, *Inorg. Chem.* 32 (1993) 898.
- [51] L.M. Vogler, K.J. Brewer, *Inorg. Chem.* 35 (1996) 818.
- [52] S. Serroni, G. Denti, *Inorg. Chem.* 31 (1992) 4251.
- [53] B.P. Sullivan, J.M. Calvert, T.J. Meyer, *Inorg. Chem.* 19 (1980) 1404.
- [54] R.P. Thummel, S. Chirayil, *Inorg. Chim. Acta* 154 (1988) 77.
- [55] C.R. Arana, H.D. Abruna, *Inorg. Chem.* 32 (1993) 194.
- [56] R.A. Krause, *Inorg. Chim. Acta* 22 (1977) 209.
- [57] K.J. Brewer, R.S. Lumpkin, J.W. Otvos, L.O. Spreer, M. Calvin, *Inorg. Chem.* 28 (1989) 4446.
- [58] L.M. Vogler, Ph.D. Dissertation, Virginia Polytechnic Institute and State University, 1995.
- [59] W.E. Jones, C.A. Bignozzi, P. Chen, T.J. Meyer, *Inorg. Chem.* 32 (1993) 1167.
- [60] J.R. Winkler, T.L. Netzel, C. Creutz, N. Sutin, *J. Am. Chem. Soc.* 109 (1987) 2381. R.M. Berger, D.R. McMillin, *Inorg. Chem.* 27 (1987) 4245.